
Bio-functionalized star PEG-coated PVDF surfaces for cytocompatibility-improved implant components

Jean Heuts,* Jochen Salber, Alexandra M. Goldyn,[†] Romy Janser,[‡] Martin Möller, Doris Klee
Institute of Technical and Macromolecular Chemistry of RWTH Aachen University and DWI at RWTH Aachen, Pauwelsstrasse 8, Aachen, D-52074, Germany

Received 31 March 2008; revised 5 November 2008; accepted 4 February 2009
Published online 8 May 2009 in Wiley InterScience (www.interscience.wiley.com). DOI: 10.1002/jbm.a.32478

Abstract: Unmodified and GRGDS peptide-modified six arm PEG star based hydrogels (Star PEG) have been applied as a multifunctional, easy to handle coating system for textile polyvinylidene fluoride (PVDF) structures, which prevent unspecific protein and cell adsorption and control-specific cell adhesion. The reactive isocyanate-terminated Star PEG has been successfully applied to ammonia-plasma treated two- and three-dimensional PVDF surfaces. Easy modification of the surface hydrogel by mixing in of GRGDS peptide during the coating step or subsequent coupling of GRGDS was determined by TOF-SIMS. Unmodified and GRGDS-functionalized hydrogel surfaces show distinct protein repellency, as demonstrated by fluorescence microscopy after incubation with fluorescent labeled proteins and Surface MALDI-TOF-

Mass Spectroscopy. Cell culture experiments with primary human dermal fibroblasts, primary fetal rat fibroblasts, and human osteoblasts on GRGDS and/or KRSR Star PEG-modified two- and three-dimensional substrates show advancement in cell adhesion and proliferation compared with untreated PVDF surfaces, whereas pure star PEG-coated surfaces show no cell adhesion. The combination of protein and cell repellent properties with specific biofunctionality and easy application of the coatings will enable their application for 3D-scaffolds. © 2009 Wiley Periodicals, Inc. *J Biomed Mater Res* 92A: 1538–1551, 2010

Key words: biocompatibility; cell adhesion; plasma; polyethylene oxide; PVDF; RGD peptide

INTRODUCTION

Tissue engineering using synthetic templates has become an emerging domain of biomedical research¹. A great deal of effort has gone into developing novel polymeric materials with improved functionality.^{2–4} Such biomaterials possess mechanical and physical properties that allow them to replace defect functions of a tissue, part of an organ, or the complete organ like, heart valves, blood ves-

sels, tendons, ligaments, etc. As biomedical devices are interfacing with biological systems, they must not initiate an adverse reaction of the organism (non-cytotoxic) but perform with an appropriate host response in their specific application.⁵ Because of the potential risk in long-term applications and the costly and time-consuming processes for the certification of newly developed polymers for implants, prostheses, and medical devices, standard polymers like poly(propylene) (PP), poly(tetrafluor ethylene) (PTFE), poly(ethylene terephthalate) (PET) and poly(dimethyl siloxane) (PDMS) are currently used in clinical long-term applications as hernia meshes, microvascular anastomotic coupling devices, artificial ligaments, and artificial vascular grafts.^{6–9} All of these polymers, however, reveal some disadvantages, for example, PET has been shown to degrade after some years, as been demonstrated for vascular grafts.^{10–13} Similarly, cases of disintegrated PET-meshes have been reported.^{14,15} PTFE as mesh material is usually manufactured in the form of foils, thus lacking a sufficient integration into the surrounding tissue.¹⁴ PP, widely used as suture material and for most mesh constructions, is rather stable in long-term applications, but shows a comparatively

*Present address: DSM Resolve, Urmonderbaan 22 (Gate 2), Geleen, 6167 RD, The Netherlands

[†]Present address: Department of Biophysical Chemistry, University Heidelberg, Im Neuenheimer Feld 253, Heidelberg, D-69120, Germany

[‡]Present address: New Mexico Institute of Mining and Technology, 801 Leroy Place, Socorro, NM 87801

Correspondence to: D. Klee; e-mail: klee@dwirwth-aachen.de

Contract grant sponsor: Fresenius Medical Care Deutschland GmbH; contract grant number: 03N4030

Contract grant sponsor: Federal Ministry of Education and Research (Germany)

high bending stiffness, resulting in rather stiff mesh prosthesis. Furthermore induction of an accentuated inflammatory foreign body reaction has been reported as a major disadvantage.^{16,17} As a particularly inert polymer having superior mechanical properties in certain applications, poly(vinylidene fluoride) (PVDF) has received much attention and generated considerable interest for use as an implant component.^{18–20} However, its performance in biomedical applications suffers from its surface properties. The surface of native PVDF is slightly negatively charged and rather hydrophobic. As a result, PVDF exhibits a strong protein affinity. Non-specific protein adsorption combined with partial or full denaturation of the protein on the foreign surface is a key step in the initiation of unwanted biological reactions of the human body. This first step in a foreign body response can lead to many problems, ranging from life threatening to merely inconvenient consequences, like acute and chronic inflammation, fibrous encapsulation, occlusion of small diameter artificial blood vessels, complement activation, biofouling combined with subsequent bacteria adhesion, proliferation of the bacteria and infection of the host, and, at last, device failure.^{21–25}

Therefore, we postulate two major also *per se* not sufficient requirements for a biomaterial. First, it should prevent unspecific adsorption of components of the blood and the interstitial fluid with the consequence of an uncontrolled stimulation of the immune system. Second, the biomaterial should direct the response of the biological system towards healing and reconstruction of the organic functions. Here the hypothesis is, that initial interfacial interactions will control to a large extent the further acceptance and healing and thus the long time performance of an implant. Hence besides general surface properties such as surface energy, surface roughness, and surface chemical composition, also time controlled specific binding and stimulation must be considered while developing advanced biomaterials.

In this report, we describe a strategy to fabricate PVDF devices with improved cell-repellent surface properties that can be functionalized with specific ligands to control adhesion, spreading, and proliferation of mesenchymal-derived cells like osteoblasts and fibroblasts. The initial activation of PVDF surfaces achieved by low-pressure microwave (MW)-induced ammonia-plasma is followed by coating the activated PVDF surfaces with Star PEG. Bioactivation with GRGDS and other ECM peptide sequences was achieved by two different strategies, simultaneously and consecutively.²⁶ All modification steps were followed by means of contact angle measurements, optical microscopy, X-ray photoelectron spectroscopy (XPS), and time-of-flight secondary ion mass spectroscopy (TOF-SIMS). Protein adsorption and repel-

lence studies were carried out by matrix-assisted laser desorption ionization time-of-flight mass spectroscopy (MALDI-TOF-MS) and fluorescent microscopy. *In vitro* cell culture experiments were started with cytocompatibility tests, using Live/Dead staining. Cell experiments were carried out with primary human osteoblasts, primary dermal fibroblasts, and fetal rat fibroblasts studying adhesion, spreading and proliferation on ultra thin ECM peptide-modified Star PEG-coated PVDF samples. Furthermore, surface modifications and cell seeding experiments were carried out on 3D PVDF textile structures. The prevention of cell adhesion on unmodified Star PEG coatings as well as cell adhesion and proliferation on ECM peptide-modified surfaces in standard cell culture media is demonstrated, independent from substrate geometry.

MATERIALS AND METHODS

Substrate materials

Glass cover slips (Marienfeld, Germany), with 15-mm diameter, were used as substrate materials. The substrates were cleaned by 5-min sonification in an Ethanol/Hexane solution [21:79] [m/m] and dried under nitrogen flow. PVDF granulate (Solvay S.A., Belgium) was used as received. PVDF meshes were manufactured by the institute for textile technology of the RWTH Aachen University (ITA). The meshes were cleaned by 4 h soxhlet extraction with an Ethanol/Hexane solution [21:79] [m/m] and dried for 1 h at 50°C.

Solvents and reagents

Six-arm star shaped NCO terminated prepolymers (Star PEG) with a backbone of statistically copolymerized 80% ethylene oxide and 20% propylene oxide ($M_n = 12,000$ g mol⁻¹, PD = 1.08) were prepared as previously described²⁷ and stored in a Unilab glove box (MBraun). The RGD peptide (GRGDS) was obtained from Bachem (Switzerland) and used as delivered. Tetrahydrofuran (THF) was dried over LiAlH₄ and distilled under nitrogen. Dimethylformamide (Fluka, 99.8%, Germany) under crown cap was used as received. Millipore water was produced by a Purelab Plus system (USF Elga, Germany). Phosphate Buffered Saline (PBS) (Sigma-Aldrich, Germany) was generated by dissolving the PBS powder in 1 L of degassed millipore water. The fluorescent marker 4-chloro-7-nitro-benzofurazan (Fluka, Switzerland) was used as received. The fluorescence-labeled proteins Avidin Texas Red and Albumin rhodamine B were obtained from the Invitrogen Corporation (US) and used as received. Lysozyme, insulin, and bovine serum albumin were obtained from Sigma-Aldrich (Germany), stored at -18°C and used as received. Syringe filters with pore size 0.2 μm were purchased from Whatman (Germany). GRGDS and KRSR peptide were

obtained from Bachem (Germany), stored at -18°C and used as received.

Spin coating of PVDF onto glass cover slips

Under nitrogen PVDF granulate was dissolved in a THF/DMF mixture [3:1] [v/v] at 80°C to gain a 0.56% solution [m/v]. For spin coating, the cleaned cover slips substrates were placed on the spin coater (Convac 1001 S, Germany) and then accelerated within 1 sec to the final rotation speed of 4500 rpm, and kept rotating for 3 min. During this time, 12 drops of filtered (syringe filter) PVDF solution are applied to the rotating substrate. After spin coating, the samples are tempered for 2 h at 160°C and 1 h at 195°C .

Ammonia-plasma treatment of two- and three-dimensional samples

Plasma treatment was carried out in a low pressure microwave plasma system AK 330 (Roth & Rau Oberflächentechnik AG, Germany). Samples were treated at a pressure of 0.4 mbar with an ammonia gas flow of 30 sccm, for a total time of 300 seconds. Three-dimensional samples (meshes) were treated for 300 seconds on both sides.

Application of diisocyanate terminated star polyethers to the two- and three-dimensional samples

Onto the two-dimensional samples, the Star PEG is spin coated. Star PEG (100 mg) is dissolved in 1 mL THF in the glove box. This solution is transferred out of the glove box and 9 mL Millipore water is added. After 5 min, the solution is filtered through a 0.2- μm syringe filter and used for spin coating. For spin coating, the plasma polymerized substrates were placed on the spin coater (Convac 1001 S, Germany) covered by the solution and then accelerated within 1 sec to the final rotation speed of 2500 rpm, and kept rotating for 40 sec. The resulting films were dried under nitrogen flow and stored over night in ambient atmosphere.

For three-dimensional samples, the star PEG is dip coated. The Star PEG solution is generated in the same way as mentioned above. After the 5-min wait, the PVDF mesh is dipped for 5 min into the Star PEG solution. Later, the samples were dried under nitrogen flow and stored for 12 h in ambient atmosphere. Subsequently, the samples were rinsed with Millipore water and dried under nitrogen flow.

Biofunctionalization of the star PEG coating with ECM peptide

Application of the GRGDS to the Star PEG coating can be done in two separate ways, incorporation during the spin or dip coating process or subsequent coupling after spin or dip coating. For incorporation, the GRGDS is dis-

solved in the used Millipore water at a concentration of $1\ \mu\text{mol mL}^{-1}$. For subsequent coupling, the samples are dip coated for 5 minutes into either a 0.1 or a 0.2 $\mu\text{mol mL}^{-1}$ GRDGDS or a 0.1/0.1 $\mu\text{mol mL}^{-1}$ GRGDS/KRSR solution in Millipore water, after the spin or dip coating application of the Star PEG. Afterwards the samples were dried under nitrogen flow and stored for 12 h in ambient atmosphere. Then the samples were rinsed with Millipore water and dried under nitrogen flow.

Contact angle measurements

Contact angle measurements were performed with a Goniometer G1 (Krüss GmbH, Germany) with Millipore water, using sessile drop and captive bubble methods. Sessile drop measurements were conducted after equilibrium of the drop on the surface was reached, typically 10 sec after drop placement. Before captive bubble measurements substrates were submerged in Millipore water for at least 8 h. Ten measurements were performed on each substrate. The resulting value of each single measurement is the average value of left and right contact angle. Errors were determined through evaluation of the standard deviation of the measurements.

Microscopy

Light microscopy and fluorescence microscopy were performed by means of an Axioplan2 Imaging microscope from Zeiss (Germany). Microscopy pictures were taken with a Zeiss AxioCam MRC5 camera. An N XBO 75 lamp from Zeiss was used as light source for fluorescence microscopy. Filter system for the NBF was filter set F41-018 from AHF analytentechnik AG (Germany), and filter system for Avidin Texas Red and Albumin rhodamine B was filter set 31 from Zeiss (Germany). Filter system for Live/Dead staining of cell culture samples was filter set 6 from Zeiss.

XPS analysis

XPS analysis of surface modified samples was performed on an AXIS Ultra spectrometer (Kratos Analytical, UK), equipped with a monochromatized Al K_{α} source. The pressure during analysis was typically 5×10^{-8} mbar. The elemental composition of samples was obtained from survey spectra, collected at a pass energy of 320 eV. Binding energies were referenced to the aliphatic carbon peak at 285.0 eV. High resolution elemental spectra were recorded at a pass energy of 40 eV. The emission angle of electrons was set at 35° with respect to the sample normal, which results in an information depth of about 10 nm.

Assessment of surface protein adsorption by fluorophore labeled proteins

Samples were half dipped into a solution of 1 g polystyrene in 50-mL toluene with a speed of $10\ \text{mm min}^{-1}$ and

withdrawn with the same speed to result a polystyrene film of 100-nm thickness (determined by ellipsometry). For dip coating, a homemade device with the motor and gearing combination 1524.A0671 from Faulhaber GmbH KG (Germany) was used. After evaporation of the solvent, the samples were immersed into a solution of 1 mg mL⁻¹ Avidin Texas Red or Albumin rhodamine B conjugate in PBS buffer for 20 min at room temperature, washed thrice with pure PBS buffer solution, thrice with Millipore water, and dried with a stream of nitrogen. Then the samples were examined by fluorescence microscopy.

Assessment of surface protein repellency by surface MALDI-TOF mass spectrometry

Lysozyme (1 mg mL⁻¹), porcine insulin (1 mg mL⁻¹), and bovine serum albumin (1 mg mL⁻¹) were dissolved in PBS buffer pH 7.4, respectively. The samples were immersed into the protein solutions at 37°C for 1 h. After washing thrice with buffer and thrice with Millipore water to remove loosely adsorbed proteins and salt, the samples were examined by means of Surface MALDI-TOF MS. Surface MALDI-TOF mass spectra were obtained using a BRUKER BIFLEXTM III MALDI time-of-flight mass spectrometer (Bruker-Franzen Analytik GmbH, Germany) equipped with a nitrogen laser (337 nm wavelength and 3 ns pulse width). Samples were placed onto the stainless steel sample holder, sinapic acid in a 0.1% solution of trifluoroacetic acid in acetonitrile/water was applied onto the sample surface, and the solvent was left to evaporate before the sample holder was inserted into the spectrometer. The adsorbed protein molecules were desorbed of the surface and embedded into the matrix crystals that formed on the samples. Pulsed laser irradiation caused volatilization and ionization of matrix crystals with the embedded proteins. Time-of-flight secondary ion mass spectrometry of Star PEG and Star PEG plus GRGDS-modified samples was carried out.

Determination of GRGDS presence in star PEG coatings by time-of-flight secondary ion mass spectroscopy

TOF-SIMS spectra were obtained using a TOF-SIMS IV instrument (Ion-TOF GmbH, Germany) with a reflectron analyzer, a cluster Bi ion source (25 keV), and a pulsed electron flood source for charge neutralization. The primary pulsed ion beam current was 1.0 pA and the primary dose was lower than 1.0 × 10¹³ ions cm⁻² (static SIMS limit). All experiments were performed using a cycle time of 100 ms (mass range 0–800 m/z). The mass spectral resolution (DM/M) was typically greater than 6000 at m/z = 27. Positive and negative ion spectra were acquired from a 100 μm × 100 μm area.

Cell culture and analysis

In vitro experiments were performed with primary human dermal fibroblasts (hdF) (patient: female, 38 years,

passage 2), primary fetal rat fibroblasts (FRF) (seven Sprague-Dawley rat fetuses, passage 2), and primary human osteoblasts (HOB) (patient: female, 35 years, passage 2). Cells were stored frozen in liquid nitrogen until usage. FRFs and hdFs were seeded into flasks in high glucose Dulbecco's modified Eagle's medium (DMEM) with supplements of 10% fetal calf serum (FCS), 1 U mL⁻¹ penicillin, and 1 mg mL⁻¹ streptomycin. Primary HOBs were cultivated in osteoblast growth media with 10% fetal bovine serum, 1% penicillin/streptomycin, and ascorbic acid 50 mg L⁻¹. Cells were grown at 37°C and humidified atmosphere containing 5% CO₂ (standard cultivation conditions). The media were changed every 2–4 days, and cells were passaged when they reached 70–80% confluence before being used for experiments. Cells of passages 4–6 were used for experiments in this study. Cells were harvested by brief exposure to 0.25% trypsin and 1 mM EDTA in PBS and seeded onto the substrate. For adhesion studies onto flat samples, a 300-μL cell suspension (hdF, FRF, and HOB) was prepared on a distinct area of the sample in a defined concentration (3 × 10⁴ cells mL⁻¹). Samples were incubated under standard cell culture conditions at 37°C, and humidified atmosphere containing 5% CO₂. Cell adherence and spreading were visualized at various times [24 h (1 day), 48 h (2 days), 120 h (5 days)] via fluorescence and/or light microscopy. Cell viability was measured with Live/Dead staining kit (Invitrogen, Germany), whereas cell morphology was visualized by hemalum staining. Before staining with hemalum, cells were fixed in 4% formalin solution (pH 7.4, PBS, 30 min) and vigorously rinsed with deionized water. For adhesion studies on surface modified PVDF meshes, three-dimensional samples were shaken in a 1 × 10⁶ cells mL⁻¹ of hdF cell suspension in histosette cassettes, under standard cell culture conditions. Samples were taken at 96-h (4 days) and 216-h (9 days) and fixed in 4% formaldehyde in PBS (pH 7.4). After vigorous washing with deionized water, samples were dehydrated and embedded in paraffin. Cell/material paraffin block was cut with a microtome in 4–5 μm slides. Sections were mounted onto glass slides and paraffin was extracted by xylol. Cells were stained by hematoxylin-eosin and visualized by light microscopy.

RESULTS AND DISCUSSION

Coating of two- and three-dimensional PVDF substrates for characterization of surface modification

Because of the fact that PVDF does not possess functional groups that allow for surface modification and its intrinsic inertness, the surface must be activated for chemical binding by a plasma treatment.^{28–33} In the presented work, two- and three-dimensional PVDF samples have been treated by low-pressure MW-induced ammonia-plasma to induce the creation of amine groups on the PVDF surface [Fig. 1(a)]. The generation of amino groups on the substrates occurs statistically. These ammonia-plasma activated

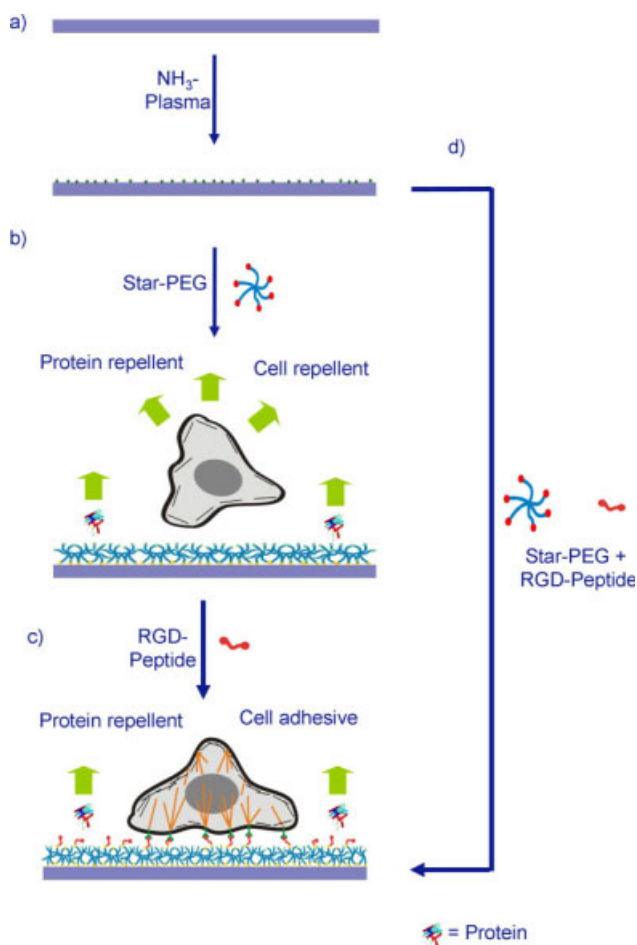


Figure 1. Idealized schematic illustration of the modification of the PVDF surface. (a) Initial activation of PVDF surfaces achieved by low-pressure microwave-induced ammonia-plasma. (b) Coating of the activated PVDF surfaces with Star PEG molecules. Biofunctionalization with GRGDS and/or KRSR peptide was achieved by two different strategies. (c) consecutively and (d) simultaneously. [Color figure can be viewed in the online issue, which is available at www.interscience.wiley.com.]

PVDF surfaces were coated with a ultrathin hydrogel in order to impede protein adsorption and cell adhesion.^{34–36} As shown in Figure 1(b,c), a densely cross-linked layer of polyethylene glycol was generated from six-armed star-shaped prepolymers with a statistically copolymerized backbone of 80% ethylene glycol and 20% propylene glycol.^{37–39} The arms are end-functionalized with isophorone diisocyanate, resulting in isocyanate-terminated prepolymers (Star PEG). These prepolymers bind covalently to the substrate by addition to the surface amino groups on the PVDF surface. Coating of the amino-functionalized PVDF substrates with Star PEG was performed by spin coating onto two-dimensional PVDF substrates or dip coating of three-dimensional PVDF meshes with an aqueous solution of the Star PEG prepolymers [Fig. 1(b)]. In this solution, water par-

tially hydrolyzes isocyanate groups to carbamic acid, which is instantly decarboxylated to form amino groups. The amino groups then react with other isocyanate groups to form a urea linkage between two arms of the star-shaped prepolymers. It is important to note that reaction of amino groups with the isocyanates is much faster than hydrolysis,⁴⁰ thus oligomerization takes place in solution. Upon immersion of the substrate, Star PEG prepolymers and oligomers react with the surface amino groups on the PVDF and covalently bind to the substrate. As the Star PEG layer remains hydrated after the coating procedure, the reaction described above finally leads to a densely crosslinked layer of urea-linked Star PEG molecules with remaining amino-functional dangling ends. These layers are homogeneous and smooth, as has been reported previously.⁴¹ Due to the slow hydrolysis of the isocyanate groups, the cross-linking process requires at least 24 h for the isocyanate groups to be completely hydrolyzed. Thus, a convenient time window remains in, which the isocyanate functionality of the surface can be used for covalent immobilization of compounds. This can be used to incorporate extracellular matrix molecules like glycoproteins or short peptides derived there of, which can bind directly to receptor proteins in the cell membrane and thus promote specific cell adherence.^{42,43} In this study, a bioactivation of the Star PEG coating for specific cell adhesion was achieved by coupling with GRGDS and/or KRSR peptide sequences by two different strategies, simultaneous coupling [Fig. 1(c)], and consecutive coupling [Fig. 1(d)]. Physicochemical characterization of all surface modification steps was conducted, along with assessment of protein repellent properties, quantitative cell proliferation on, and cytocompatibility tests on two- and three-dimensional PVDF samples. Two different types of primary fibroblasts, h4F and FRF, were used to investigate the cytocompatibility of the described surface coatings. FRFs were chosen for improved transferability of cell culture results to *in vivo* biocompatibility test with Sprague Daley rats. Furthermore HOBs adherence was studied for surfaces equipped with the osteoblasts specific sequence KRSR.⁴⁴ As the cell adherence promotion of the GRGDS and KRSR peptides have already been mentioned in literature and also have been found by the authors in previous studies, it was chosen not to incorporate GRDGS or similar scrambled peptides as controls in this study.^{26,37}

Physicochemical characterization

Surface modifications and coating quality were assessed by contact angle measurements, optical microscopy, XPS, and TOF-SIMS.

TABLE I
XPS Elemental Composition (in At. %), Bond Energies and Fractions of Carbon (C1s) Species of: a) Pure PVDF, b) Ammonia Plasma-Treated PVDF, c) Star PEG-Coated PVDF Surfaces, d) Consecutively Bio Activated Star PEG Surface, e) Simultaneously Bio Activated Star PEG Surface

Sample	Atom-%	C1s in Atom-%						
		285,0	286,5	287,7	290,5	O1s	N1s	F1s
		C—H C—C	C—O C—N	R—C=O O—C—O	CF ₂ O—CO—O			
a) PVDF	46,4	23,9	—	—	22,5	1,5	—	52,1
b) NH ₃ -Plasma	71,6	54,6	5,1	4,8	7,1	5,8	1,9	20,6
c) Star PEG coating	73,0	18,8	54,2	—	—	24,7	1,5	0,9
d) Star PEG + GRGDS	73,4	26,1	47,3	—	—	23,3	2,0	1,3
e) Star PEG + GRGDS	71,9	16,7	55,2	—	—	24,5	1,8	1,8

To determine surface wettability the water contact angle of unmodified and modified PVDF two-dimensional substrates was determined in sessile drop and captive bubble mode. A pure unmodified PVDF surface shows a contact angle of 69° in sessile-drop mode and an angle of 68° in captive-bubble mode. After ammonia-plasma treatment, contact angles drop to 42 (sessile drop) and 45 (captive bubble). Subsequent coating of the plasma-treated PVDF surface with Star PEG and biofunctionalization of the Star PEG coating by subsequent or simultaneous coupling of GRGDS peptide onto the surface produced values in a range of 41–43° for sessile-drop mode and 40–41° for captive-bubble mode. There were no statistically significant differences in contact angle between pure Star PEG coatings and with GRGDS biofunctionalized Star PEG coatings. These values correlated with previously determined values for water contact angles on Star PEG coatings.⁴⁵

To verify the surface modification steps, XPS experiments were carried out on two- and three-dimensional unmodified and surface-modified PVDF samples. Table I shows the elemental composition and carbon bond energy of approximately the outermost 10 nm of the uncoated PVDF surface, the ammonia-plasma-treated PVDF surface and Star PEG as well as biofunctionalized Star PEG coated two-dimensional PVDF surfaces. Pure PVDF shows an elemental composition, which is consistent with the expected theoretical composition of 50% carbon and 50% fluor content. After ammonia-plasma treatment, carbon, oxygen, and nitrogen content increased to respectively 71.6, 5.8, and 1.9%. The fluor content of the surface decreased from 52.1 to 20.6%. Additionally, more and higher energetic carbon species were detected after plasma treatment. It is well known that upon ammonia-plasma treatment of polymers, the formation of amino groups and other nitrogen containing groups is concurrent with oxidative processes. Both processes, the introduction of N into the PVDF surface as well as the partial oxidation, are

confirmed by the XPS data presented here. The occurrence of amine groups after ammonia-plasma treatment has been found by authors in previous studies, for instance, by causing the surface to react with an amine-reactive fluorescent dye: 4-chloro-7-nitrobenzofurazane after ammonia-plasma treatment.⁴⁶ After coating of the plasma-treated PVDF surface with Star PEG and biofunctionalization of the Star PEG coating by subsequent or simultaneous coupling of GRGDS peptide and subsequent coupling of KRSR peptide onto the surface typical values of surface atomic content for Star PEG coatings were detected.⁴¹ There were no significant differences detected between pure Star PEG coatings and with GRGDS/KRSR biofunctionalized Star PEG coatings. The amount of detected fluor on the Star PEG modified surface decreased massively to 1.8% or less. XPS measurements on unmodified and modified three-dimensional PVDF textile structures showed similar results.

To detect small amounts of GRGDS peptide in the top most 2 nm of the biofunctionalized Star PEG coatings TOF-SIMS measurements were carried out on a pure Star PEG coating and a Star PEG coating biofunctionalized by the coupling of 1.0 μmol mL⁻¹ GRGDS simultaneously during the coating. Figure 2 shows positive and negative TOF Static SIMS spectra recorded on pure and biofunctionalized Star PEG coatings. Cationic and anionic fragments, which were only present on the biofunctionalized coatings and were indicative for the presence of GRGDS peptide in the uppermost 2 nm of the coating, are listed.

Characterization of surface protein repellency

Protein repellent properties of the Star PEG and biofunctionalized Star PEG coatings were further examined. Therefore, two-dimensional Star PEG-coated PVDF samples were halfway dipped into a polystyrene (PS) solution to yield samples, that were

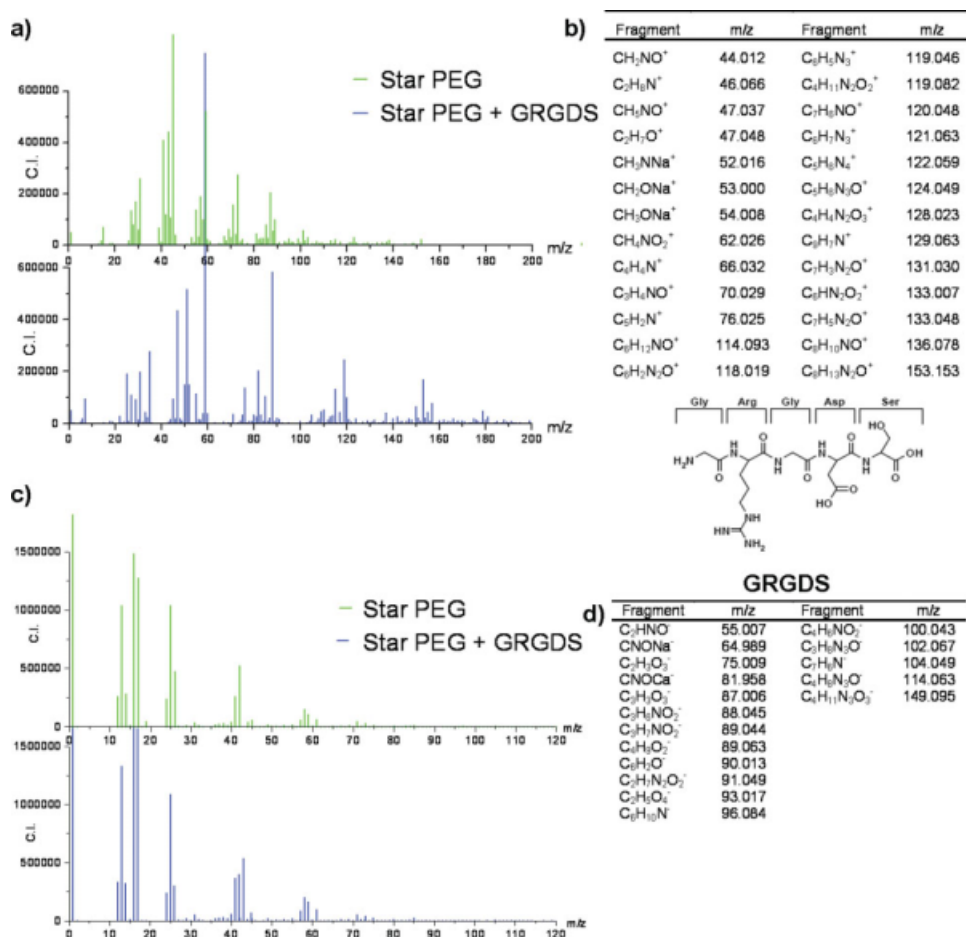


Figure 2. (a) Positive TOF Static SIMS spectra recorded on Star PEG and bioactivated Star PEG + GRGDS surface, (b) Cationic fragments indicative for GRGDS presence on the bioactivated Star PEG + GRGDS surface, (c) Negative TOF Static SIMS spectra recorded on Star PEG and bioactivated Star PEG + GRGDS surface, and (d) Anionic fragments indicative for GRGDS presence on the bio activated Star PEG + GRGDS surface. [Color figure can be viewed in the online issue, which is available at www.interscience.wiley.com.]

half covered by PS, a hydrophobic compound known to induce protein adsorption.⁴⁷ Adsorption of Avidin Texas Red conjugate and albumin rhodamine B conjugate was analyzed by means of fluorescence microscopy. Representative fluorescence microscopy images are presented in Figure 3. In all cases, the protein adsorbs on the PS, which results in a high fluorescence intensity, whereas the biofunctionalized Star PEG-coated sample areas on the two-dimensional samples do not show fluorescence intensity higher than the background intensity, indicating the lack of adsorbed protein. Unmodified and Star PEG-modified three-dimensional PVDF textile structures were incubated with Avidin Texas Red conjugate. Representative fluorescence microscopy images are presented in Figure 3. Pure PVDF three-dimensional textile structures required very short exposure times of 300 ms. Star PEG-coated and biofunctionalized Star PEG-coated three-dimensional textile structures required exposure times in a range of 17–20 sec. The need to use a short exposure time (300 ms) to get a

clear fluorescence microscopy picture of the textile structure indicates that a large amount of fluorescent protein is present on the surface. After Star PEG coating of the surface one needs a large exposure time to amass the necessary light to generate a clear picture of the Star PEG-coated structure. This signifies that a very small amount of fluorescing protein is present on the Star PEG-coated structure. This indicates a significant improvement of protein repellence after coating with Star PEG.

The ability of the Star PEG and biofunctionalized Star PEG coatings to repel insulin as well as albumin was assessed by Surface-MALDI-TOF mass spectrometry. Insulin was chosen as a model protein because of its relatively small size (M_w 5778 Da) and spheroid shape to test the density of the PEG coating on the surface. Albumin was chosen as a model protein because of its relatively high concentration in the blood and bodily fluids and its tendency to be the first protein to adsorb onto a foreign material surface introduced into the body. Furthermore, they

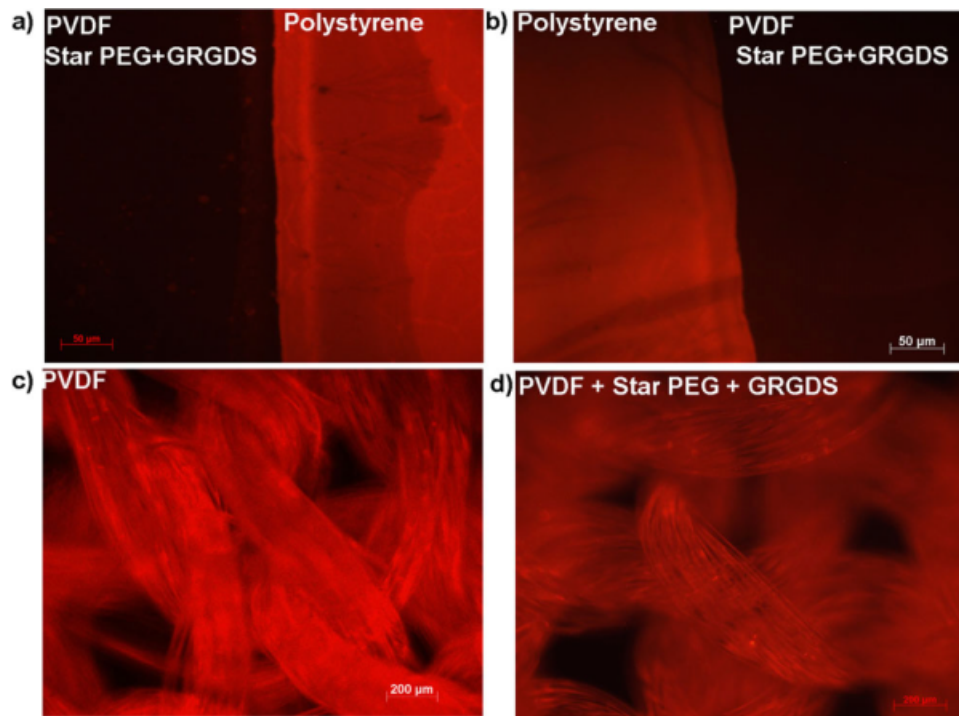


Figure 3. Fluorescence microscopy with fluorophore labeled proteins on two-dimensional samples (a) with Avidin Texas Red conjugate on a biofunctionalized Star PEG + GRGDS surface and a polystyrene reference surface, (b) with albumin rhodamine B conjugate on a biofunctionalized Star PEG + GRGDS surface and a polystyrene reference surface. On three-dimensional PVDF textile structures with Avidin Texas Red conjugate, (c) pure PVDF with an exposure time of 300 ms, and (d) biofunctionalized Star PEG + GRGDS with an exposure time of 17 sec.

have Surface-MALDI-TOF-MS that detects small amounts of material but is difficult to quantify.^{25,48} Figure 4 shows surface-MALDI-TOF-MS spectra from surfaces incubated with insulin (left-hand side) and albumin (right-hand side). Insulin could only be

detected on pure PVDF and ammonia-plasma-treated PVDF surfaces. Albumin could only be detected on the pure PVDF surface. On Star PEG and biofunctionalized Star PEG coatings no insulin and albumin could be detected.

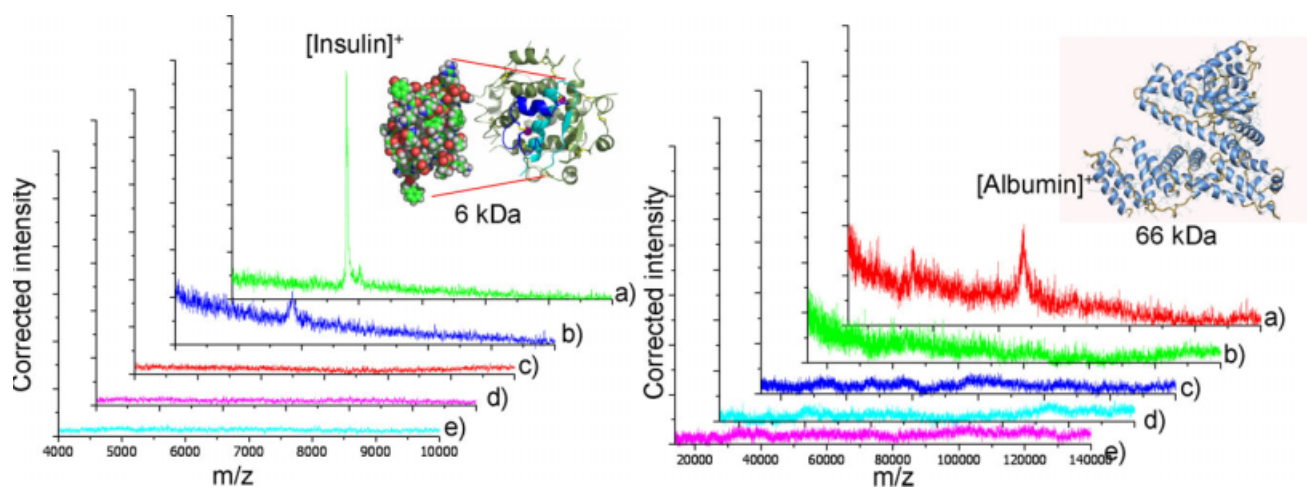


Figure 4. Surface-MALDI-TOF mass spectra of insulin (left hand side) and albumin (right hand side) on (a) pure PVDF, (b) ammonia plasma treated PVDF, (c) Star PEG-coated PVDF, (d) Star PEG-coated PVDF biofunctionalized by consecutive coupling of $0.1 \mu\text{mol mL}^{-1}$ of GRGDS, and (e) Star PEG-coated PVDF biofunctionalized by mixing in $1.0 \mu\text{mol mL}^{-1}$ of GRGDS, during the coating step.

Cell proliferation on and cytocompatibility tests of two- and three-d-dimensional PVDF structures

Figure 5 presents the results of static cell-culture experiments with primary hdF, FRF, and HOB cells on two-dimensional PVDF samples. Figure 5(a) shows cell adhesion values of hdF cells on the various modified surfaces and controls. No values for pure unmodified Star PEG coatings are displayed in Figure 5, as no cells adhered to them in the 24, 48, and 72 h time periods. As to be expected, cell adhesion and proliferation on tissue culture poly styrene (TCPS) control surfaces was very good. After 72 h, the number of adherent hdFs on TCPS was over 100%, indicating that the 96 well bottoms were as completely covered and that cells started to grow into the third dimension. Cell adhesion and proliferation on the native unmodified PVDF surface was low. Although of comparable wettability, TCPS and unmodified PVDF surfaces exhibited different hdF adhesion and proliferation characteristics.^{1,33} After ammonia-plasma treatment of the PVDF surface, initial adhesion of the hdF cells was quite low (24, 48 h), whereas the proliferation on the plasma-treated PVDF surface was very good with adherent cell values after 72 h, reaching the same cell density as for the TCPS control after 72 h. The high adherent cell value reached after 72 h on ammonia-plasma-treated PVDF is believed to be due to the introduction of oxygen- and nitrogen-containing functional groups into the PVDF surface by the ammonia plasma, which is understood to be very beneficial for cell proliferation.⁴⁹ As previously described, a coating of pure Star PEG resulted in no hdF adhesion, as also shown in Figure 6(g,i). An introduction of GRGDS peptide in concentrations of 0.1 or 0.2 $\mu\text{mol mL}^{-1}$ by consecutive coupling onto the Star PEG coating [Fig. 1(c)] resulted in both low cell adhesion and low proliferation. A concentration of 0.1 $\mu\text{mol mL}^{-1}$ was therefore sufficient for a low initial specific cell adhesion onto the surface, which induced a subsequent hdF proliferation and homogeneous seeding of the surface after 72 h. An increase in concentration to 0.2 $\mu\text{mol mL}^{-1}$ GRGDS peptide neither influenced the amount of initial adhered cells, nor the proliferation rate. An introduction of GRGDS peptide in a higher concentration of 1.0 $\mu\text{mol mL}^{-1}$ through simultaneous coupling of the peptide during the Star PEG coating process [Fig. 1(d)] produced a surface, which showed a significantly increased hdF adhesion and proliferation as compared to the consecutive immobilization of GRGDS. In case of the Star PEG coatings with simultaneously immobilized GRGDS peptide, it is believed that the increased initial adhesion is promoted by the higher density of the GRGDS peptide on the coated surface. An advantage of simultaneous cou-

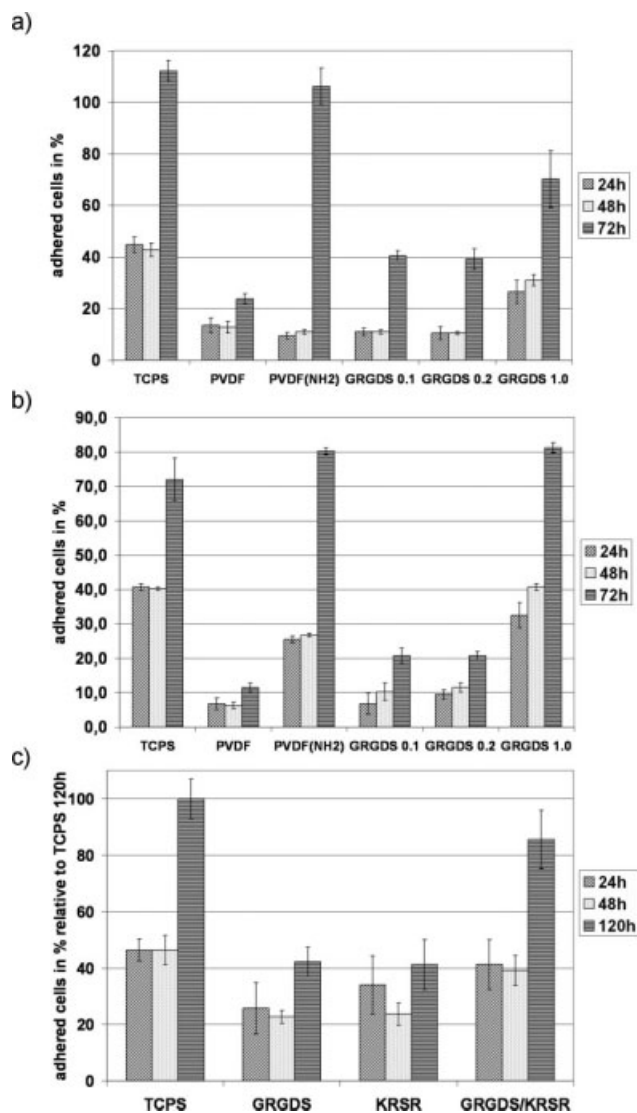


Figure 5. Adherent cells on TCPS control, unmodified, ammonia-plasma treated, Star PEG and biofunctionalized Star PEG-coated PVDF surfaces. The adherent cell numbers after 24 h show initial adhesion; the cell numbers after 72/120 h area measure for cell proliferation. Adherent cell numbers for (a,b) are shown relative to a determined confluent cell mat. Adherent cell numbers for (c) are shown relative to the TCPS 120 h control. No values for pure unmodified Star PEG coatings are shown as no cells adhere to them. a: hdF adherence on TCPS control and PVDF samples with 0.1, 0.2 $\mu\text{mol mL}^{-1}$, consecutively and 1.0 $\mu\text{mol mL}^{-1}$, simultaneously coupled GRGDS on Star PEG. b: FRF adherence on TCPS control and PVDF samples with 0.1, 0.2 $\mu\text{mol mL}^{-1}$, consecutively and 1.0 $\mu\text{mol mL}^{-1}$ simultaneously coupled GRGDS peptide. d: HOB adherence on TCPS control and 0.1 $\mu\text{mol mL}^{-1}$ GRGDS, 0.1 $\mu\text{mol mL}^{-1}$ KRSR and a mixture of 0.1 $\mu\text{mol mL}^{-1}$ GRGDS and 0.1 $\mu\text{mol mL}^{-1}$ KRSR consecutively coupled to the Star PEG coating.

pling method is the easy control over the peptide sequence to Star PEG molecule ratio just by the amount of peptide added to the water phase prior to mixing with the star prepolymer molecules in THF.³⁷ However, a disadvantage of the simultaneous

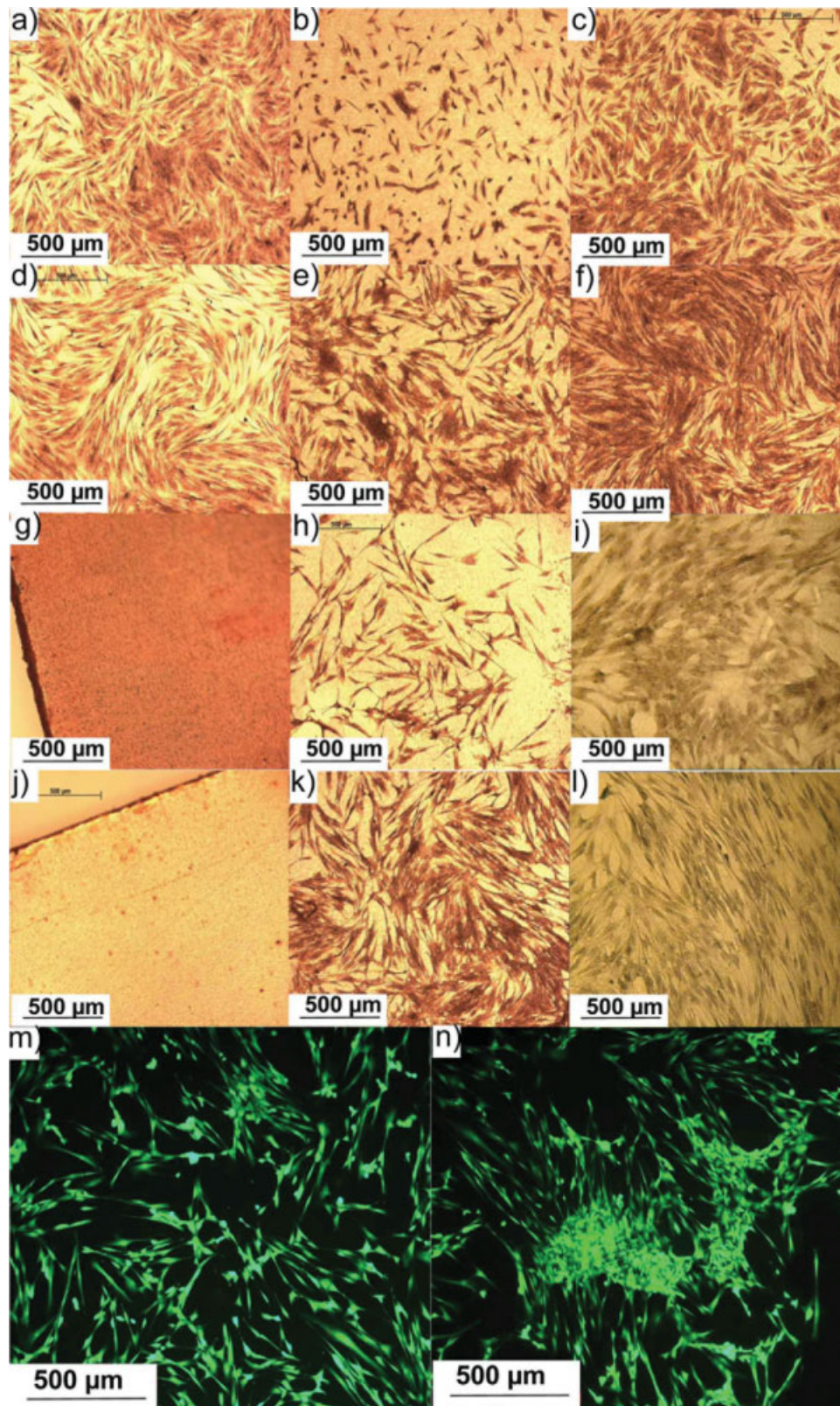


Figure 6. Examples for adherent human dermal fibroblasts on TCPS controls, unmodified and modified PVDF two-dimensional surfaces. Hemalum staining of TCPS control after (a) 24 h (d) 48 h. Native PVDF surface after (b) 24 h, (e) 72 h. Ammonia- plasma- treated PVDF surface after (c) 24 h, (f) 48 h. Star PEG-treated PVDF surface after (g) 24 h, (j) 72 h. $0.1 \mu\text{mol mL}^{-1}$ GRGDS coupled consecutively to Star PEG coating after (h) 24 h, (k) 48 h. $1.0 \mu\text{mol mL}^{-1}$ GRGDS coupled simultaneously during Star PEG coating after (i) 24 h, (j) 48 h. Live/Dead staining of $0.1 \mu\text{mol mL}^{-1}$ GRGDS coupled consecutively to Star PEG coating after (m) 24 h, (n) 48 h. [Color figure can be viewed in the online issue, which is available at www.interscience.wiley.com.]

peptide coupling method is the need to use higher peptide concentrations, due to the fact that a certain amount of the peptide is located in the coating inaccessible for the cells and their receptors. This might be not acceptable for implant modifications, especially when longer and more expensive peptide sequences will be used. Here the consecutive coupling method could be advantageous.

The similarity of the cell adhesion values after 24 and 48 h is believed to be due to the arresting of the cells in G_0 phase caused by the trypsination procedure used to harvest the cells, before being applied to the tested surface. This effect is described in literature.⁵⁰ However, cell spreading is increased after 48 h (Fig. 6).

As seen in Figure 6, hdfFs are adhered but show lower spreading on unmodified PVDF in comparison to TCPS and ammonia-plasma-treated PVDF after 24 h. Furthermore, cell spreading and hdfF density on the surface are comparable for the TCPS control and ammonia-plasma-treated PVDF after 48 h. Pure Star PEG coatings resulted in no hdfF adhesion, as shown in Figure 6(g,h). Consecutive coupling of $0.1 \mu\text{mol mL}^{-1}$ GRGDS onto the Star PEG coating gives a similar amount of initially adhered cells after 24 h in comparison to unmodified PVDF, but as shown in Figure 6(i) cell spreading is much better. After 48 h, hdfFs demonstrate an increase in cytoplasm/nucleus ratio and a slight increase in adherent cell numbers for this particular area of sample surface. Additionally, Live/Death stainings confirm the typical fibroblast morphology and demonstrate that all adhered cells are viable and not negatively influenced by the surface coating. Figure 6(k,l) show the increased initial cell adhesion, spreading, and a higher proliferation rate due to the increased GRGDS presence on the surface.

Figure 5(b) shows equivalent initial adhesion and proliferation characteristics of FRFs as compared to hdfFs. Cell test micrographs (not shown) of FRFs demonstrate behavior similar to hdfFs on all surfaces.

Several studies have demonstrated improved cell attachment, proliferation, and spreading by modifying materials with integrin-binding peptide sequences.⁴³ Recently, an increasing number of studies have shown that proteoglycan-binding domains of several cell adhesion mediating proteins can modulate cell spreading and stress fiber formation in different cell types.^{51,52} Thus, it is believed that cell surface proteoglycans cooperate with integrins in regulating maximal cell adhesion and spreading.⁵³ Indeed, a few studies have demonstrated improved cell attachment and spreading using both integrin and proteoglycan-binding domains to biofunctionalize biomaterial surfaces.^{54,55} In this study, we pursued this strategy to biofunctionalize PVDF-Star PEG surfaces with the reported proteoglycan-binding

peptide KRSR⁵⁶ alone and in combination with GRGDS peptide. We hypothesized that the peptide combination would stimulate cell-binding and spreading above that of single-peptide couplings. Figure 5(c) illustrates the initial adherence and proliferation behavior of HOBs on TCPS controls and Star PEG coatings consecutively coupled with either $0.1 \mu\text{mol mL}^{-1}$ GRGDS, $0.1 \mu\text{mol mL}^{-1}$ KRSR, or a mixture of $0.1 \mu\text{mol mL}^{-1}$ GRGDS and $0.1 \mu\text{mol mL}^{-1}$ KRSR. As is to be expected, initial HOB adhesion and proliferation on TCPS control surfaces is good. Coupling of a single peptide, either GRGDS or KRSR shows moderate initial adherence and low proliferation behavior, whereas the combination of GRGDS and KRSR demonstrates good initial adherence (24 h) and proliferation (120 h) of the HOBs. This indicates that osteoblasts adhesion is mediated by different receptor types. The RGD sequence is known to promote cell adhesion via the Integrin $\alpha_5\beta_1$ and the KRSR sequence is specific for osteoblasts adhesion via proteoglycan-based receptors.⁵⁷ This causes synergy effects, which amplify adhesion and proliferation of HOBs.^{56,58}

Live/Death stainings of HOBs on Star PEG coatings consecutively coupled with either $0.1 \mu\text{mol mL}^{-1}$ GRGDS, $0.1 \mu\text{mol mL}^{-1}$ KRSR, or a mixture of $0.1/0.1 \mu\text{mol mL}^{-1}$ GRGDS/KRSR surfaces, are shown in Figure 7. Here an increase in cell number and cell clustering for the GRGDS/KRSR surface is seen as opposed to the single GRGDS and KRSR surfaces after 48 h. As observed in the 120 h micrographs of the central area of the investigated samples, osteoblasts are distributed homogeneously and show good adhesion, viability, and spreading

Conversely, in another study Dettin et al. observed that a combination of RGD/KRSR did not increase osteoblast adhesion on TCPS, in comparison to surfaces modified with only RGD or KRSR.⁵⁴ This demonstrates impressively, that not only bioligand-type or bioligand-mixture influences the cell/biomaterial-surface interaction, but also surface-bioligand concentration, character of bioligand-presentation, and finally its bioavailability seem to be important as well.^{26,37,59} Another critical point is that most studies performed only short-term cultivation experiments with osteoblasts.⁶⁰ Here, we cultivated HOBs on PVDF-Star PEG-GRGDS, PVDF-Star PEG-KRSR, and PVDF-Star PEG-(GRGDS/KRSR) for 120 h. Finally, enhanced HOB spreading was observed on all three peptide-modified PVDF-Star PEG surfaces [Fig. 7(b,d,f)].

Figure 8 illustrates long-term cell culture experiments with human fibroblasts on Star PEG-coated three-dimensional PVDF monofilament meshes. After 4 days, no cell adhesion and proliferation is seen on hemalum stained histological cross-sections of pure Star PEG-coated PVDF meshes [Fig. 8(a)]. After 9 days, cell adhesion and proliferation on pure Star

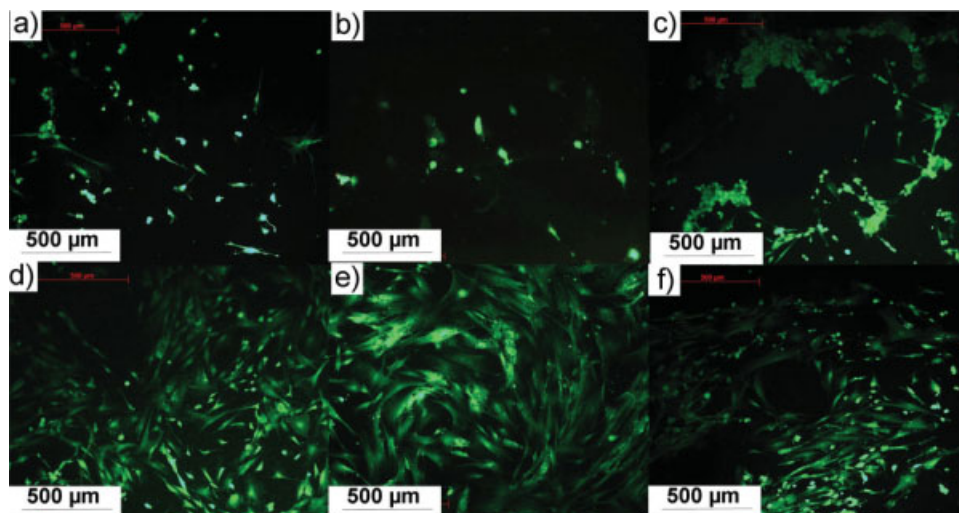


Figure 7. Determination of cell viability of human osteoblasts by Live/Dead staining of $0.1 \mu\text{mol mL}^{-1}$ GRGDS coupled consecutively to Star PEG coating after (a) 48 h, (b) 120 h. Of $0.1 \mu\text{mol mL}^{-1}$ KRSR coupled consecutively to Star PEG coating after (c) 48 h, (d) 120 h. Of a mixture of $0.1 \mu\text{mol mL}^{-1}$ GRGDS and $0.1 \mu\text{mol mL}^{-1}$ KRSR coupled consecutively to Star PEG coating after (e) 48 h, (f) 120 h. [Color figure can be viewed in the online issue, which is available at www.interscience.wiley.com.]

PEG-coated PVDF meshes was very minor. An introduction of $0.1 \mu\text{mol mL}^{-1}$ GRGDS onto the Star PEG coating by consecutive coupling gives good hDF adherence after 4 days [Fig. 8(c)] and good cell proliferation onto and around the PVDF monofilaments after 9 days. PVDF monofilament meshes coated with GRGDS peptide in a higher concentration of $1.0 \mu\text{mol mL}^{-1}$ through simultaneous coupling of the

peptide during the Star PEG coating process [Fig. 1(d)] produced a surface, which showed an even more increased hDF adhesion and proliferation rate after 4 and 9 days, as compared to the consecutive immobilization of GRGDS. These results confirm the transferability of the coatings with good quality from two-dimensional samples to three-dimensional PVDF monofilament meshes. The easy application of

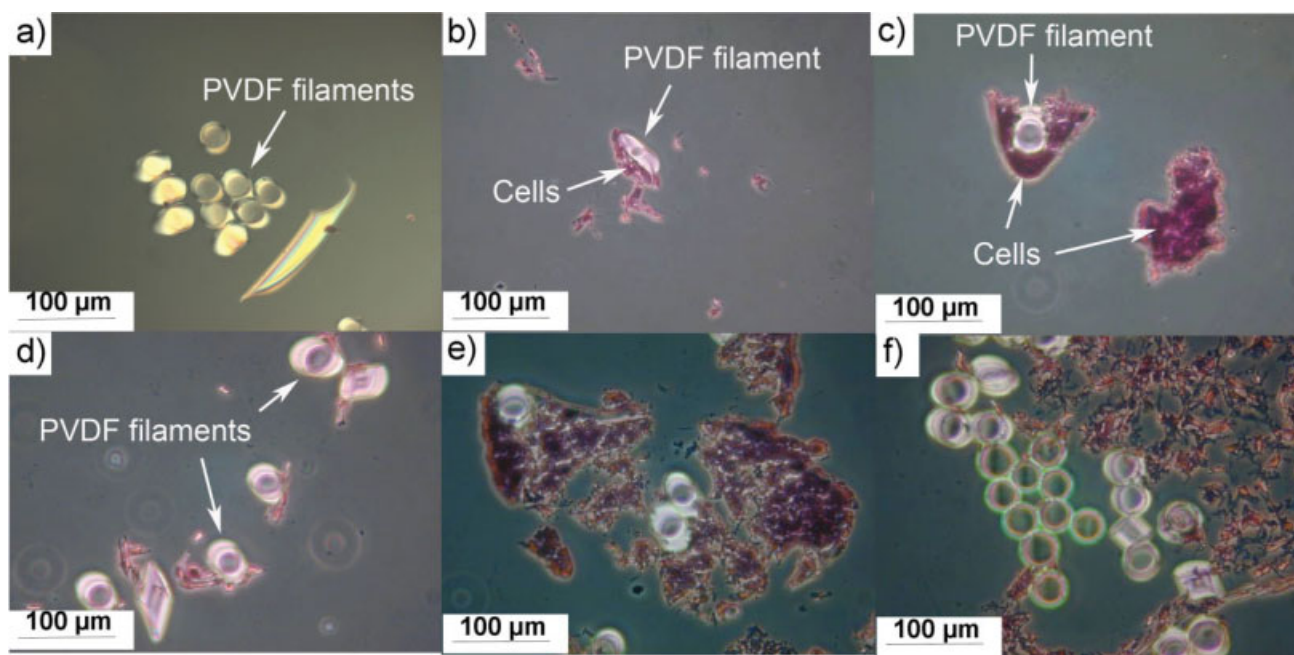


Figure 8. Examples for adhesion and proliferation of human dermal fibroblast on PVDF monofilament meshes. Star PEG-coated PVDF after (a) 4 days, (d) 9 days. $0.1 \mu\text{mol mL}^{-1}$ GRGDS coupled consecutively to Star PEG coated PVDF after (b) 4 days, (e) 9 days. $1.0 \mu\text{mol mL}^{-1}$ GRGDS coupled simultaneously during Star PEG-coated PVDF after (c) 4 days, (f) 9 days. [Color figure can be viewed in the online issue, which is available at www.interscience.wiley.com.]

the Star PEG coatings as well as the combination of protein and cell repellent properties and their specific biofunctionality provides large potential for further applications in surface modification of three dimensional-scaffolds for implantation.

CONCLUSIONS

The development of a coating system for two- and three-dimensional PVDF substrates, which is protein repellent, cell repellent, and able to be biofunctionalized for specific cell adhesion, has been presented. Successful immobilization of ECM peptide sequences was determined by TOF-SIMS. Furthermore, protein repellency of the unmodified and biofunctionalized Star PEG coatings was assessed by Surface MALDI-TOF-MS and microscopy of fluorescent labeled proteins. Cells were viable on the biofunctionalized Star PEG coatings as determined by Live/Death staining. The easy application of the Star PEG coatings, as well as the combination of protein repellent and cell repellent properties and their ability to be specifically biofunctionalized by either simultaneously or consecutively coupling of cell adhesive peptide sequences provides large potential for further applications in surface modification of three-dimensional PVDF scaffolds for implantation. Especially, the ability to target specific cells for adhesion by implementing cell adhesive mediators, particular for a single cell class, in the hydrogel coating, and the ability to create cell repellent and specific cell adhesive domains on a single implant (e.g., for a smart artificial tendon prosthesis) hold much promise.

The authors thank Prof. Helmut Thissen of CSIRO Molecular and Health Technologies (Melbourne, Australia), Dr. Grant van Riessen and Dr. Narelle Brack of Latrobe University (Melbourne, Australia) for their assistance with the TOF-SIMS measurements.

References

1. Tsuruta T. Contemporary topics in polymeric materials for biomedical applications. *Adv Polym Sci* 1996;126:1–51.
2. Klee D, Höcker H. Polymers for biomedical applications: Improvement of the interface compatibility. *Adv Polym Sci* 1998;149:1–57.
3. Langer R, Tirrell DA. Designing materials for biology and medicine. *Nature* 2004;428:487–492.
4. Lendlein A, Kratz K, Kelch S. Smart implant materials. *Med Device Technol* 2005;16:12–14.
5. Ratner BD, Hoffman AS, Schoen FJ, Lemons JE, editors. *Biomaterials Science, An Introduction to Materials in Medicine*. San Diego: Elsevier; 2004.
6. Schumpelick V, Junge K, Rosch R, Klinge U, Stumpf M. Retromuscular mesh repair for ventral incision hernia in Germany. *Chirurg* 2002;73:888–894.
7. Devine C, McCollum C. Heparin-bonded Dacron or polytetrafluoroethylene for femoropopliteal bypass: Five-year results of a prospective randomized multicenter clinical trial. *J Vasc Surg* 2004;40:924–931.
8. Zaffagnini S, De Pasquale V, Montanari C, Strocchi R, Maccacii M. Histological and ultrastructural evaluation of Leeds-Keio ligament six years after implant. A case report. *Knee Surg Sports Traumatol Arthrosc* 1997;5:89–94.
9. Trail IA, Martin JA, Nuttall D, Stanley JK. Seventeen-year survivorship analysis of silastic metacarpophalangeal joint replacement. *J Bone Joint Surg Br* 2004;86:1002–1006.
10. Vinard E, Eloy R, Descotes J, Brudon JR, Guidicelli H, Magne JL, Patra P, Berruet R, Huc A, Chauchard J. Stability of performances of vascular prostheses; retrospective study of 22 cases of human implanted prostheses. *J Biomed Mater Res* 1988;22:633–648.
11. Maarek JM, Guidoin R, Aubin M, Prud'homme RE. Molecular weight characterization of virgin and explanted polyester arterial prostheses. *J Biomed Mater Res* 1984;18:881–894.
12. Berger K, Sauvage LR. Late fiber deterioration in Dacron arterial grafts. *Ann Surg* 1981;193:477–491.
13. Riepe G, Loos J, Imig H, Schroder A, Schneider E, Petermann J, Rogge A, Ludwig M, Schenke A, Nassutt R, Chakfe N, Morlock M. Long-term in vivo alterations of polyester vascular grafts in humans. *Eur J Vasc Endovasc Surg* 1997;13:540–548.
14. Schumpelick V, Kingsnorth G. *Incisional Hernia of the Abdominal Wall*. Berlin: Springer; 1999.
15. Leber GE, Garb JL, Alexander AI, Reed WP. Long-term complications associated with prosthetic repair of incisional hernias. *Arch Surg* 1998;133:378–382.
16. Klinge U, Klosterhalfen B, Conze J, Limberg W, Obolenski B, Öttinger AP, Schumpelick V. Shrinking of polypropylene mesh in vivo: An experimental study in dogs. *Eur J Surg* 1998;164:965–969.
17. Klinge U, Klosterhalfen B, Öttinger AP, Junge K, Schumpelick V. PVDF as a new polymer for the construction of surgical meshes. *Biomaterials* 2002;23:3487–3493.
18. Laroche G, Marois Y, Guidoin R, King MW, Martin L, How T, Douville Y. Polyvinylidene fluoride (PVDF) as a biomaterial: From polymeric raw material to monofilament vascular suture. *J Biomed Mater Res* 1995;29:1525–1536.
19. Lynen Jansen P, Klinge U, Anurov M, Titkova S, Mertens PR, Jansen M. Surgical mesh as a scaffold for tissue regeneration in the esophagus. *Eur Surg Res* 2004;36:104–111.
20. Junge K, Rosch R, Klinge U, Kronen C, Klosterhalfen B, Mertens PR, Lynen P, Kunz D, Preiss A, Peltroche-Llacsahuanga H, Schumpelick V. Gentamicin supplementation of polyvinylidene fluoride mesh materials for infection prophylaxis. *Biomaterials* 2005;26:787–793.
21. Tang L, Jennings TA, Eaton JW. Mast cells mediate acute inflammatory responses to implanted biomaterials. *Proc Natl Acad Sci U S A* 1998;95:8841–8846.
22. Johnson R, Harrison D, Tucci M, Tsao A, Lemos A, Puckett A, Hughes JL, Benghuzzi H. Fibrous capsule formation in response to ultrahigh molecular weight polyethylene treated with peptides that influence adhesion. *Biomed Sci Instrum* 1997;34:47–52.
23. Bos GW, Scharenborg NM, Poot AA, Engbers GH, Beugeling T, van Aken WG, Feijen JJ. Blood compatibility of surfaces with immobilized albumin-heparin conjugate and effect of endothelial cell seeding on platelet adhesion. *J Biomed Mater Res* 1999;44:330–340.
24. Kidane A, Park K. Complement activation by PEO-grafted glass surfaces. *J Biomed Mater Res* 1999;44:640–647.
25. Kingshott P, St. John HA, Griesser HJ. Direct detection of proteins adsorbed on synthetic materials by matrix-assisted laser desorption ionization-mass spectrometry. *Anal Biochem* 1999;273:156–162.

26. Salber J, Gräter S, Harwardt M, Hofmann M, Klee D, Dujic J, Jinghuan H, Ding J, Kippenberger S, Bernd A, Groll J, Spatz JP, Möller M. Influence of different ECM mimetic peptide sequences embedded in a nonfouling environment on the specific adhesion of human-skin keratinocytes and fibroblasts on deformable substrates. *Small* 2007;3:1023–1031.
27. Götz H, Beginn U, Bartelink CF, Grünbauer HJ, Möller M. Preparation of diisocyanate terminated star polyethers. *Macromol Mater Eng* 2002;287:223–230.
28. Ikada Y. Blood-compatible polymers. *Adv Polym Sci* 1984;57:103–140.
29. Liston EM, Martinu L, Wertheimer MR. Plasma surface modification of polymers for improved adhesion: A critical review. *J Adhes Sci Technol* 1993;7:1091–1127.
30. Gengenbach TR, Xie X, Chatelier RC, Griesser HJ. Evolution of the surface composition and topography of perfluorinated polymers following ammonia-plasma treatment. *J Adhes Sci Technol* 1994;8:305–328.
31. Kang ET, Zhang Y. Surface modification of fluoropolymers via molecular design. *Adv Mat Weinheim* 2000;12:1481–1494.
32. Ademovic Z, Klee D, Kingshott P, Kaufmann R, Höcker H. Minimization of protein adsorption on poly(vinylidene fluoride). *Biomol Eng* 2002;19:177–182.
33. Klee D, Ademovic Z, Bosserhoff A, Höcker H, Maziolis G, Erli HJ. Surface modification of poly(vinylidene fluoride) to improve the osteoblast adhesion. *Biomaterials* 2003;24:3663–3670.
34. Lee KY, Mooney DJ. Hydrogels for tissue engineering. *Chem Rev* 2001;101:1869–1877.
35. Drury JL, Mooney DJ. Hydrogels for tissue engineering: Scaffold design variables and applications. *Biomaterials* 2003;24:4337–4351.
36. Harris JM. Poly(ethylene glycol) chemistry: Biotechnical and Biomedical Applications. New York: Plenum Press; 1992.
37. Groll J, Fiedler J, Engelhard E, Ameringer T, Tugulu S, Klok HA, Brenner RE, Moeller M. A novel star PEG-derived surface coating for specific cell adhesion. *J Biomed Mater Res* 2005;74A:607–617.
38. Amirgoulova EV, Groll J, Heyes CD, Ameringer T, Röcker C, Möller M, Nienhaus GU. Biofunctionalized polymer surfaces exhibiting minimal interaction towards immobilized proteins. *ChemPhysChem* 2004;5:552–555.
39. Groll J, Amirgoulova EV, Heyes CD, Ameringer T, Röcker C, Nienhaus GU, Möller M. Biofunctionalized, ultrathin coatings of cross-linked star-shaped poly(ethylene oxide) allow reversible folding of immobilized proteins. *J Am Chem Soc* 2004;126:4234–4239.
40. Caraculacu AA, Coseri S. Isocyanates in polyaddition processes. Structure and reaction mechanisms. *Prog Polym Sci* 2001;26:799–851.
41. Groll J, Ademovic Z, Ameringer T, Klee D, Moeller M. A comparison of coatings from reactive star shaped PEG-stat-PPG prepolymers and grafted linear PEG for biological and medical applications. *Biomacromolecules* 2005;6:956–962.
42. Shin H, Jo S, Mikos AG. Biomimetic materials for tissue engineering. *Biomaterials* 2003;24:4385–4415.
43. Hersel U, Dahmen C, Kessler H. RGD modified polymers: Biomaterials for stimulated cell adhesion and beyond. *Biomaterials* 2003;24:4385–4415.
44. Dettin M, Conconi MT, Gambaretto R, Bagnola A, Di Bello C, Mentib AM, Grandib C, Parnigotto PP. Effect of synthetic peptides on osteoblast adhesion. *Biomaterials* 2005;26:4507–4515.
45. Groll J, Ameringer T, Spatz JP, Moeller M. Ultrathin Coatings from Isocyanate-Terminated Star PEG Prepolymers: Layer formation and Characterization. *Langmuir*, 2005;21:1991–1999.
46. Klee D, Heuts J, Salber J, Groll J, Möller M. Biofunctional Star PEG coatings on 3 dimensional polyvinylidene fluoride scaffolds for specific cell adhesion. *Trans Ann Meet Soc Biomat* 2007;32:214.
47. Kanaya S, Crouch R. DNA sequence of the gene coding for *Escherichia coli* ribonuclease H. *J Biol Chem* 1983;258:1276–1281.
48. Kingshott P, John S, Chatelier RC, Griesser H. Matrix-assisted laser desorption ionization mass spectrometry detection of proteins adsorbed in vivo onto contact lenses. *J Biomed Mat Res* 2000;49:36–42.
49. Mitchell SA, Poulsson AHC, Davidson MR, Emmison N, Shard AG, Bradley, Cellular attachment and spatial control of cells using micro-patterned ultra-violet/Ozone treatment in serum enriched media, *Biomaterials*. 2004;25:4079–4086.
50. Nasmyth K. A prize for proliferation. *Cell* 2001;107:689–701.
51. Woods A, McCarthy JB, Furcht LT, Couchman JR. A synthetic peptide from the carboxy-terminal heparin-binding domain of fibronectin promotes focal adhesion formation. *Mol Biol Cell* 1993;4:605–613.
52. Dalton BA, McFarland CD, Underwood PA, Steele JG. Role of the heparin binding domain of fibronectin in attachment and spreading of human bone-derived cells. *J Cell Sci* 1995;108:2083–2092.
53. Couchman JR, Woods A. Syndecan-4 and integrins: Combinatorial signaling in cell adhesion. *J Cell Sci* 1999;112:3415–3420.
54. Dettin M, Conconi MT, Gambaretto R, Pasquato A, Folini M, Di Bello C, Parnigotto PP. Novel osteoblast-adhesive peptides for dental/orthopedic biomaterials. *J Biomed Mater Res* 2002;60:466–471.
55. Sagnella S, Anderson E, Sanabria N, Marchant RE, Kottke-Marchant K. Human endothelial cell interaction with biomimetic surfactant polymers containing peptide ligands from the heparin binding domain of fibronectin. *Tissue Eng* 2005;11:226–236.
56. Dee KC, Andersen TT, Bizios R. Design and function of novel osteoblast-adhesive peptides for chemical modification of biomaterials. *J Biomed Mater Res* 1998;40:371–377.
57. Damsky CH. Extracellular matrix-integrin interactions in osteoblast function and tissue remodeling. *Bone* 1999;25:95–96.
58. Aplin AE. Cell adhesion molecule regulation of nucleocytoplasmic trafficking. *FEBS Lett* 2003;534:11–14.
59. Gasteier P, Reska A, Schulte P, Salber J, Offenhausser A, Moeller M, Groll J. Surface grafting of PEO-based star-shaped molecules for bioanalytical and biomedical applications. *Macromol Biosci* 2007;7:1010–1023.
60. Reznia A, Healy KE. Integrin subunits responsible for adhesion of human osteoblast-like cells to biomimetic peptide surfaces. *J Orthop Res* 1999;17:615–623.